

Reflection physics in X-ray-emitting Symbiotic Stars

Jesús A. Toalá^{*} 

Universidad Nacional Autónoma de México, Instituto de Radioastronomía y Astrofísica, Antigua Carretera a Pátzcuaro 8701, Ex-Hda. San José de la Huerta, Morelia 58089, Michoacán, Mexico

5 January 2024

ABSTRACT

X-ray-emitting symbiotic stars exhibit a variety of spectral shapes classified as α , β , γ , δ and β/δ types, which have been attributed to different phenomena such as thermonuclear burning on the surface of the white dwarf (WD) component, shocks between winds and jets with the red giant companion’s extended atmosphere, the presence of heavily extinguished hot plasma from the inner region from an accretion disk and/or a combination of these. However, there is observational evidence that this classification scheme is not definite and, for example, some sources change from one type to another within months or years. In this work, it is proposed that a simple disk-like model can be used to explain the X-ray properties observed from reflection dominated symbiotic stars. For this purpose we use the Stellar Kinematics Including Radiative Transfer (SKIRT) code, which has been recently upgraded to include radiative transfer from X-ray photons. It is found that the properties of the accretion disk (geometry and density) in combination with the viewing angle can be invoked to explain the spectral properties of β , δ and β/δ X-ray-emitting symbiotic stars. Spectral variations and type swaps observed for some X-ray-emitting sources can also be explained by variations in the disk properties.

Key words: (stars:) binaries: symbiotic — accretion, accretion discs — X-rays: stars — X-rays: binaries

1 INTRODUCTION

X-ray emission from symbiotic stars has been typically used to probe accretion physics. In such systems, material from a mass-losing red giant is accreted onto a white dwarf (WD; Mukai 2017)¹. It is still not clear what is the exact process in which the accretion onto the WD is powered (Bondi-Hoyle process, a Roche-lobe overflow or a wind Roche-lobe overflow channel; Bondi & Hoyle 1944; Podsiadlowski & Mohamed 2007), but the formation of an accretion disk is expected in some sources. In fact, evidence of accretion disks has been confirmed in the X-ray regime thanks to the detection of iron lines in the 6.0–7.0 keV energy range (e.g., Eze 2014). The 6.7 and 6.97 keV emission lines correspond to the He- and H-like Fe emission by hot plasma, whilst the 6.4 keV is produced by reflection of hard X-ray photons from the WD or the accretion disk (see Ishida et al. 2009). Nevertheless, these emission lines are not detected in all symbiotic stars.

Mürset et al. (1997) presented an early scheme to classify symbiotic stars based on *ROSAT* X-ray spectra, which had a relatively soft spectral range of 0.1–2.4 keV. α -type are assigned to extremely soft sources ($E < 0.4$ keV), and are usually attributed to thermonuclear burning on the surface of the WD (Orio et al. 2007), β -type symbiotic stars peak at ~ 0.8 keV and are explained by the presence of optically thin plasma with temperatures of $\sim 10^6$ K likely produced by winds

and/or jets, but resolved in only a few sources (see, e.g., Kellogg et al. 2001, 2007; Toalá et al. 2022). Finally, the γ -type was assigned to sources that exhibited spectra harder than 1.0 keV, but it is now accepted that these sources might host neutron stars instead of WD accreting sources (see, e.g., Merc et al. 2019).

Nevertheless, with the advent of the subsequent generation of X-ray instruments it became clear that symbiotic stars emit hard X-ray photons, up to 100 keV (Kennea et al. 2009). A fourth category (δ -type) was introduced by Luna et al. (2013) and corresponds to highly-absorbed, hard X-ray-emitting sources, with a clear presence of the Fe emission lines in the 6.0–7.0 keV energy range. In addition, Luna et al. (2013) introduced the β/δ -type which was assigned to sources that exhibit properties of those both types.

1.1 Reflection models for X-ray-emitting Symbiotic Stars

While the (α , β , γ , δ , β/δ) classification scheme is straightforward, it is not definitive. For example, the recurrent symbiotic star T CrB evolved from a δ -type as detected by *Suzaku* 2006 observations (Luna et al. 2008) into a β/δ -type by 2017 when *XMM-Newton* re-observed it just after it started a high period of activity (Luna et al. 2018; Zhekov & Tomov 2019). On the other hand, HM Sge was initially classified as a β -type with a simple spectrum dominated at 0.8 keV (see fig. 3 in Mürset et al. 1997), but the 2016 *XMM-Newton* observations detected a new soft component ($E < 0.5$ keV) which was attributed to shocked plasma with a temperature of $\gtrsim 3 \times 10^5$ K, very likely produced by a 100 km s^{-1} jet detected in optical wavelengths (Corradi et al. 1999). This demonstrates that HM Sge can no longer be classified as a β -type symbiotic star (see Toalá, Botello & Sabin 2023). In addition, it might be also due to detection limits of the

^{*} E-mail: j.toala@irya.unam.mx

¹ A more general definition of a symbiotic star has been proposed in the literature by Luna et al. (2013), where other compact objects (neutron stars or stellar black holes) accrete material from a red giant companion. In this paper we will refer to symbiotic stars as those hosting a WD.

instrument. For example, R Aqr was classified as an α -type source in the original work of Mürset et al. (1997), but it can be classified as a β/δ -type after being observed with the current generation of X-ray satellites (see appendix in Toalá et al. 2023). The highly variable nature of symbiotic stars suggest the classification scheme is misleading, thus questioning our understanding of the X-ray emission from symbiotic systems and encourage us to look for a more fundamental scenario to explain the diversity of X-ray spectra. This situation become more difficult if one takes into account that only about 60 symbiotic systems have been detected in X-rays among the almost 300 that have been confirmed in our Galaxy².

It is worth mentioning here the similarity between the X-ray spectra of symbiotic stars and those of active galactic nuclei (AGN), where reflection physics has been found to be important. Good-quality X-ray spectra of β/δ -type symbiotic systems are very similar to those of AGN as earlier pointed out by Wheatley & Kallman (2006). These authors compared the ASCA spectrum of the β/δ -type system CH Cyg with those of Seyfert 2 galaxies arguing that the X-ray spectrum of symbiotic systems should be dominated by scattering by an ionised medium. Wheatley & Kallman (2006) tried to model the soft component of the X-ray spectrum of CH Cyg as a result of scattering of the hard plasma from a photoionised medium around its WD component. Wheatley & Kallman (2006) used the *absori* model included in XSPEC (Arnaud 1996), but it does not allow to define a specific geometry for the absorber (see also Wheatley et al. 2003).

Other authors have attempted models including reflection from disks. For example, Ishida et al. (2009) used the *reflect* model (Magdziarz & Zdziarski 1995), originally tailored for AGN and adopted a thin distribution of material (a slab) in which reflection from neutral material is produced. Reflection naturally produces the 6.4 keV Fe emission line without the need to include an independent (and arbitrary) Gaussian component in the spectral fit.

Building over the multi-instrument and multi-epoch X-ray data of CH Cyg, Toalá et al. (2023) corroborated that indeed a reflection component is needed to unambiguously fit the 2.0-4.0 keV energy range of the *XMM-Newton* spectrum of this source in addition to the 6.4 keV Fe fluorescent line. However, the reflection component is not enough to fit the softer range (below 2.0 keV) and low-extinction thermal plasma are needed. These properties confirm that the physics behind the production of X-ray emission in symbiotic stars is tightly correlated with the reflection physics.

This paper is aim to peer at the reflection physics produced by the presence of an accretion disk around the WD component. We want to assess the impact produced by different parameters on the observed X-ray spectra of symbiotic stars and their variability. This paper is organised as follows. In Section 2 we describe the methodology used in this work. Our results are presented in Section 3. The discussion and conclusions are presented in Sections 4 and 5, respectively.

2 METHODS

For the experiments presented here, we used the Stellar Kinematics Including Radiative Transfer (*skirt*; version 9.0; Camps & Baes 2020) code. *skirt* is a Monte Carlo radiative transfer code that models the effects of absorption, scattering and re-emission from a source into a predefined medium. It has been widely-used to model the

² See the statistics in the New Online Database of Symbiotic Variables: <https://astronomy.science.upjs.sk/symbiotics/statistics.html>

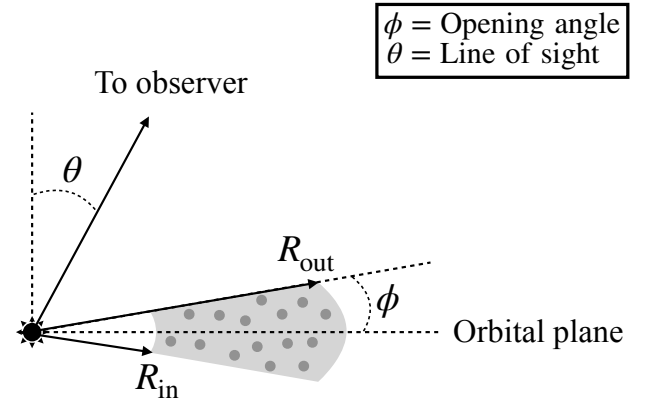


Figure 1. Illustration of the geometric scheme (a flared disk) used in our *skirt* simulations. R_{in} and R_{out} are the inner and outer radii, ϕ defines the opening angle and θ is the line of sight angle towards the observer.

CSM around supermassive black holes in AGN (see, e.g., González-Martín et al. 2023; Trayford et al. 2017, and references therein) and has been recently extended to include the treatment of X-ray photons by including the effects of Compton scattering on free electrons, photo-absorption and fluorescence by cold atomic gas, scattering on bound electrons and extinction by dust (Vander Meulen et al. 2023).

Simulations of accreting WDs predict complex toroidal-like density structures around the binary systems (see for example de Val-Borro et al. 2009; Makita et al. 2000; Liu et al. 2017; Lee et al. 2022; Saladino et al. 2019). More specifically, simulations of the accretion on a WD in a symbiotic system presented by Lee et al. (2022) predict flared accretion disks with radius of a few times 0.1 AU. And on the other hand, in the work of Liu et al. (2017) the density distribution of gas around the binary system accumulates into toroidal-like structures with external radii of hundreds of AU, depending on the different mass-accretion efficiencies and specific angular momentum which are consequences of the mass ratio of the stars in the binary system.

To illustrate the effects of reflection from the medium around symbiotic stars, we will use a simple distribution of material. Reflection calculations using results obtained from detailed hydrodynamical simulations will be presented in a subsequent paper. *skirt* allows the user to define a number of built-in geometries and here we have selected a flared disk characterised by inner (R_{in}) and outer (R_{out}) radii, and opening angle ϕ as illustrated in Fig. 1. The flared disk is also characterised by an averaged column density N_{H} . A standard value of $N_{\text{H}} = 5 \times 10^{23} \text{ cm}^{-2}$ is used in the calculations unless specified differently. The models presented here adopt a clumpy distribution for the flared disk with clump radii of 0.01 AU and a total number of clumps of 3000 stochastically distributed in the disk. The temperature of the disk is adopted to be 10^4 K, that is, completely ionised. The disk clump properties and temperature will not changed during any of the calculations presented here. All of the models are run adopting a distance of 1 kpc, consequently, they are not meant to reproduce any specific object.

Another input parameter required in *skirt* is the ionising source and its properties. In works addressing the AGN properties, the input source is defined as a power law which is related to the comptonization process in such systems (Magdziarz et al. 1998; Done et al. 2012) and the same approach was adopted by Ishida et al. (2009) for

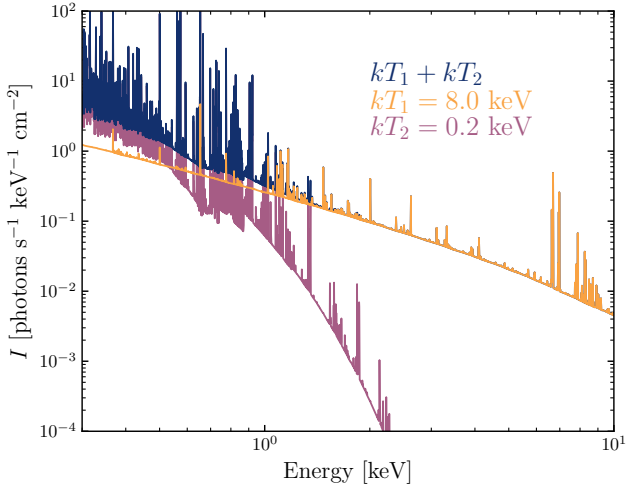


Figure 2. Examples of thermal components ($kT_1=8.0$ keV and $kT_2=0.2$ keV) generated with `xSPEC`. These plasma models are examples of plasma components used as input parameters in the `skIRT` simulations. The dark blue line shows the addition of the two $kT_1=8.0$ keV and $kT_2=0.2$ keV plasma components.

the case of the dwarf nova SS Cyg. However, thus far, there is not evidence of a similar process taking place in symbiotic stars. X-ray studies of δ - and β/δ -type symbiotic stars suggest at the presence of heavily absorbed, high temperature optically-thin component (Luna et al. 2013). It is very likely that such emission is generated at the boundary layer between the inner edge of the accretion disk and the WD. Matter is transferred from the disk, loosing its keplerian motion energy, which is deposited on the surface of the WD. This plasma has been estimated to have temperatures in the 10^5 – 10^8 K range depending on the effectiveness of the accretion rate (Pringle & Savonije 1979; Patterson & Raymond 1985), where low plasma temperatures are associated with high accretion rates and vice versa.

In line with such predictions, the calculations presented here adopt a shocked plasma model as the input source of X-ray photons, assuming that the source of X-ray photons is the boundary layer. However, in our models the source of X-ray photons is adopted to be a point source at the center of the grid. A plasma temperature of $kT_1=8$ keV ($T_X \approx 9.3 \times 10^7$ K) is adopted in most of the calculations (unless specified otherwise), more or less consistent with the hot plasma components reported in other X-ray studies of symbiotic systems (e.g., Ishida et al. 2009; Luna et al. 2013; Mukai et al. 2007; Toalá et al. 2023). An input table was calculated making use of the `apec` model³ in `xSPEC` adopting solar abundances with no extinction (this effect is consistently calculated by `skIRT`). This thermal model is illustrated in Fig. 2 with a yellow line. For comparison and discussion we also computed other `apec` plasma models with temperatures between 0.1 keV ($\approx 10^6$ K) and 20 keV ($\approx 2.3 \times 10^8$ K). The 0.2 keV emission model is also plotted alongside the 8.0 keV `apec` model in Fig. 2. All of the calculations were performed adopting an X-ray luminosity for the `apec` models of $L_X = 2 \times 10^{33}$ erg s⁻¹ for the 0.3–10.0 keV energy range.

³ <https://heasarc.gsfc.nasa.gov/xanadu/xspec/manual/XSmodelApec.html>

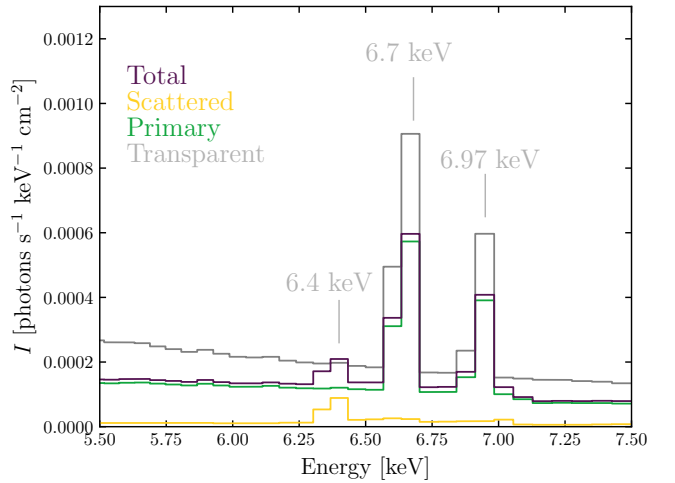
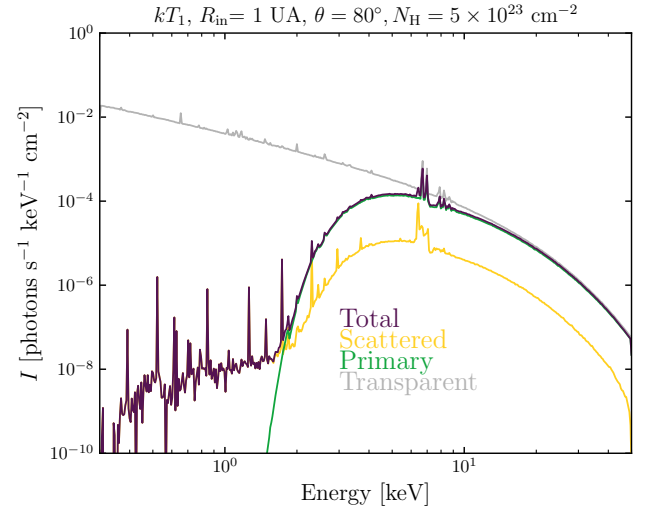


Figure 3. Resultant components for a `skIRT` simulation with standard parameters ($kT_1=8.0$ keV, $R_{in}=1$ AU, $R_{out}=200$ AU, $N_H = 5 \times 10^{23}$ cm⁻², $\phi = 30^\circ$ and $\theta = 80^\circ$). The bottom panel shows a zoom at the three Fe emission lines.

3 RESULTS

3.1 Overall properties

To illustrate the capabilities of `skIRT`, Fig. 3 presents results from a simulation adopting our standard parameters: $kT_1=8.0$ keV, $R_{in}=1$ AU, $R_{out}=200$ AU, $N_H = 5 \times 10^{23}$ cm⁻² and $\phi = 30^\circ$. These results were computed adopting a line of sight of $\theta=80^\circ$. This figure illustrates the different components reported by `skIRT`: the transparent (or unabsorbed) flux, the absorbed spectrum from the primary source, the scattered spectrum produced by the disk and the total resultant spectrum. Fig. 3 illustrates the 0.3–50.0 keV energy range that can be compared with *Chandra*, *XMM-Newton* and *Suzaku* observations. The bottom panel of this figure zooms into the 5.5–7.5 keV energy range to show that the 6.4 keV is purely produced by the scattered component, whilst the 6.7 and 6.79 keV Fe emission lines are a consequence of the hot plasma.

It is worth noticing here that a thermal plasma component produces similar results as adopting a power law distribution as input model. As a consequence, the emission detected at high energies in all of

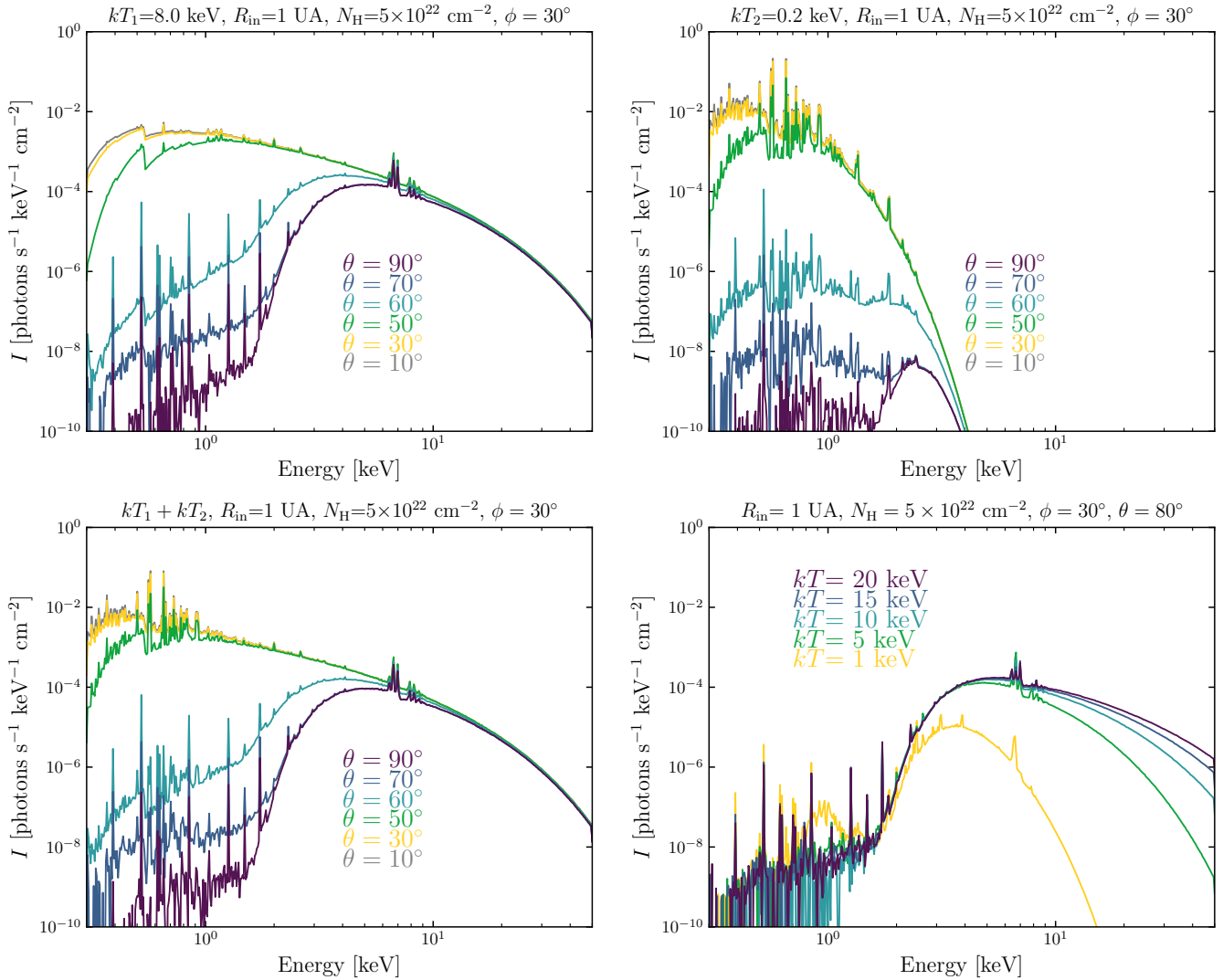


Figure 4. Reflection spectra obtained with `SKIRT` by varying the line of sight θ . The top, middle and bottom panels show results from adopting input plasma temperatures of $kT_1 = 8.0$ keV, $kT_2 = 0.2$ keV and $kT_1 + kT_2$. In all cases $R_{\text{in}}=1$ AU, $R_{\text{out}}=200$ AU, $N_{\text{H}} = 5 \times 10^{23} \text{ cm}^{-2}$ and $\phi = 30^\circ$.

our models is thermal in nature. This suggests that accreting, X-ray-emitting systems are able to produce hard X-ray emission even in the absence of magnetic fields.

A large number of `SKIRT` simulations was performed to study the dependence on the different parameters. Models varying R_{in} , θ , ϕ , N_{H} and kT were performed. We note that varying R_{out} did not result in significantly different synthetic spectra. Thus, this parameter has been kept fixed in all of our calculations. Further results are presented in the following subsection.

3.2 Effects of viewing angle

We started the `SKIRT` simulations by evaluating the effect of the viewing angle. The top-left panel of Fig. 4 presents simulations of the standard model changing the viewing angle θ from 10° to 90° for models with a single plasma temperature of $kT_1=8$ keV. This panel shows that as soon as the inclination angle is large enough ($\theta > 50^\circ$ for this set of models), the disk absorbs most of the soft X-ray emission. As a consequence, the synthetic spectra resemble

those of δ -type symbiotic stars with negligible contribution from the soft X-ray range (see for example the case of RT Cru and Hen 3-461; Luna & Sokolowski 2007; Luna et al. 2013).

The synthetic spectra of models with large θ values predict some emission for energies below 2 keV, but it is so marginal that real X-ray observations might miss it depending on the exposure time, the observed count rate and distance to the source. This simple experiment confirms that the reflection component produced by the disk plays a major role in shaping the observed spectra of symbiotic stars.

3.3 Temperature behaviour

The top-right panel of Fig. 4 presents similar calculations but adopting a plasma temperature of $kT_2 = 0.2$ keV as input model. Naturally, these models do not produce significant emission harder than 3 keV. This panel shows that as soon as the line of sight is increased, absorption plays an important role in reducing the total observed flux. Simply because soft photons are more easily absorbed than hard X-ray emission. High θ values reduce considerably the total observed

flux. These experiments show that soft sources (high-accreting systems) will be difficult to be detected for large θ values (close to edge-on geometries).

The bottom-left panel of Fig. 4 shows calculations assuming that the central source emits as a two-temperature plasma emission model, the same hard component of $kT_1 = 8.0$ keV with an extra contribution from a soft temperature of $kT_2 = 0.2$ keV. The effect of the soft component is appreciated as an excess of emission lines in the 0.3–1.0 keV energy range, best seen for small θ values (see bottom panel of Fig. 4), but this is no longer important for $\theta > 50^\circ$. In fact, there are almost no differences between models in the top-left and bottom-left panels of Fig. 4 for large θ values. Again, this is purely due to the fact that the soft X-ray emission is easily absorbed by the disk material in the line of sight. The top-right and bottom-left panels of Fig. 4 suggest that in those sources that soft X-ray emission is detected, either we are looking close to pole-on directions or the soft emission corresponds to extended emission located outside the disk, where extinction is negligible.

The bottom-right panel of Fig. 4 illustrates the impact of using a harder plasma component. The first thing to notice is that a plasma model with $kT_1=1$ keV is not able to produce the 6.4 keV Fe fluorescent line, which is only present for larger input temperature models. The emission from the 6.97 keV Fe emission line dominates models with larger kT_1 values given that is a higher ionisation stage. To illustrate the changes in the flux of the Fe emission lines with temperature we show in Fig. A1 a zoom of the 5.5–7.5 keV energy range of this panel (see Appendix A). Finally, we note that the increase of the plasma temperature is reflected in the slope of the continuum for energies > 10 keV. Larger input plasma produce larger flux at higher energies. Higher input plasma temperatures will thus result in high hardness ratio values.

3.4 The impact of the disk properties

Fig. 5 presents results of varying other parameters such as R_{in} (top panel), ϕ (middle panel) and N_{H} (bottom panel). Varying R_{in} produced almost no difference between models for small θ (not shown here), but these are only significant for high θ values. For example, Fig. 5 top panel shows that for $\theta = 80^\circ$ the resultant soft ($E < 2.0$ keV) X-ray emission is increased by increasing R_{in} . That is, the disk is narrower and less material absorbs soft photons.

The middle panel of Fig. 5 shows that the variation of the opening angle ϕ produces similar effects as varying the viewing angle. Large opening angles approximate to a spherical shell structure around the X-ray-emitting source, which are less likely under the accretion disk scenario.

Finally, the bottom panel of Fig. 5 shows the effects of increasing the disk column density N_{H} . Same as in the previous cases, the reduction of the soft X-ray emission by absorption is increasing by higher N_{H} values. However, the most interesting feature of this panel is the change in the flux of the Fe emission lines. Particularly note the variation of the fluorescent line in comparison with those produced by the ionised plasma. A model with $N_{\text{H}} = 1 \times 10^{25} \text{ cm}^{-2}$ is able to completely extinguish the contribution from the 6.7 keV Fe line. The ratio of the 6.7 keV Fe line over that of the 6.4 keV line increases by reducing N_{H} . A figure showing a zoom of the 5.5–7.5 keV energy range illustrating this situation is also presented in Appendix A.

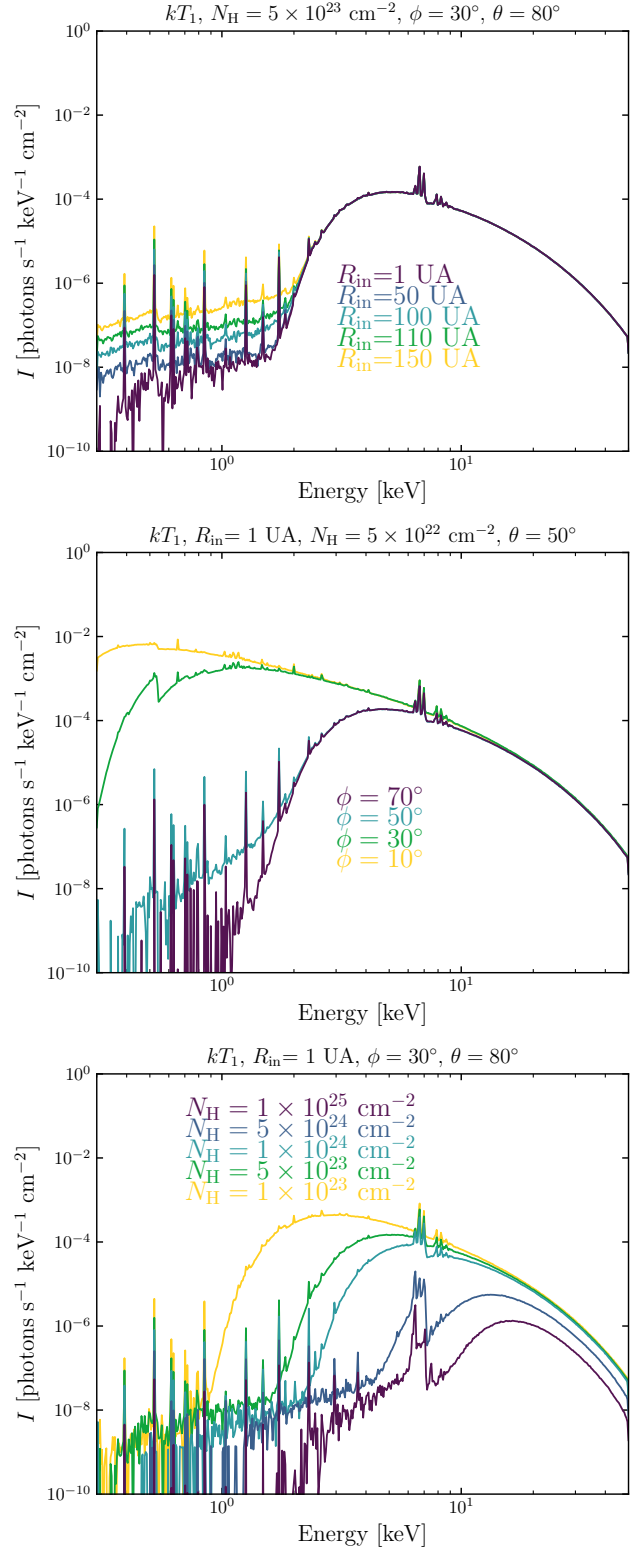


Figure 5. Reflection spectra of flared disks obtained from our *skIRT* simulations varying the inner radius R_{in} (top left), the opening angle ϕ (top right), the column density N_{H} (bottom left) and the input plasma temperature kT_1 (bottom right).

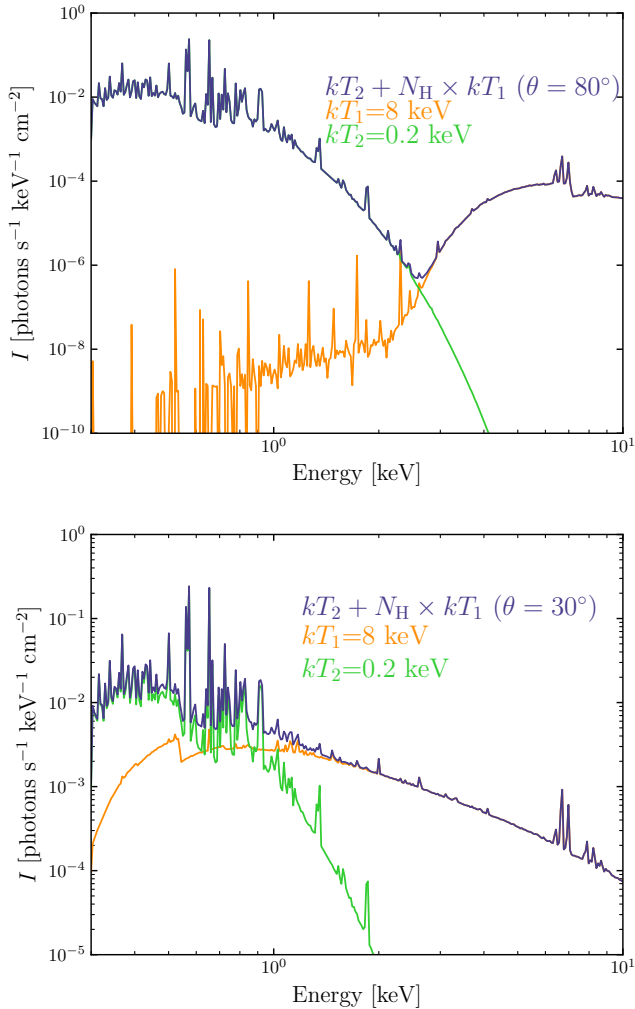


Figure 6. Two component skIRT models. The top panel shows a hard component ($kT_1=8.0$ keV) that has been processed through a flared disk model with $\theta = 80^\circ$ as in Fig. 3 while the soft component ($kT_2=0.2$ keV) has not been extinguished. The bottom panel presents the same model but with $\theta = 30^\circ$.

4 DISCUSSION

It is currently difficult to argue that all symbiotic systems might form an accretion disk, however, in those that is formed, it must definitely have an impact on the X-ray properties as demonstrated here. A relatively simple flared disk model can be used to explain the variety of X-ray properties detected from δ - and β/δ -type symbiotic stars, the reflection dominated systems. A disk model including reflection of X-ray photons from a relatively hot source naturally produces the 6.4 keV fluorescent emission line as also discussed by other authors in the past (see, e.g., Toalá et al. 2023, and references therein), but reflection is rarely used when fitting X-ray spectra of symbiotic stars. More importantly, we showed that reflection from a highly-extinguished, shocked hot plasma causes similar effects as that of a power law model (non thermal in origin) for the input source (see Ishida et al. 2009), usually done for AGN.

Close to edge-on viewing angles naturally produce δ -type X-ray-emitting symbiotic stars, very similar to the observed ones (e.g., Luna & Sokoloski 2007). Our simulations show that δ -type symbiotic

systems not only require the reflection component seen though a close to edge-on disk-like structure, but this needs to be produced by relatively hot plasma temperatures ($kT \gtrsim 1$ keV). That is, δ -type sources are very likely associated with low-accreting systems.

Including a two-temperature plasma emission model as input does not produce spectra similar to those reported for β/δ symbiotic stars where at least two temperature plasma models are needed: *i*) a hot ($kT=5\text{--}20$ keV) and heavily extinguished ($N_H \gtrsim 10^{23}$ cm $^{-2}$) component and *ii*) the contribution from a soft ($\lesssim 0.2$ keV) plasma with a low column density ($N_H \approx 10^{20}$ cm $^{-2}$, very likely due to Galactic column densities). For example, those of CH Cyg, NQ Gem, V347 Nor, ZZ CMi (see Mukai et al. 2007; Luna et al. 2013; Toalá, Botello & Sabin 2023). That is, the soft component of β/δ -type sources can not be physically located near the symbiotic system if the spectrum is dominated by reflection as demonstrated in Fig 4. To illustrate the possible situation of β/δ sources, Fig. 6 presents calculations of a reflection model with typical values used here and convolved with the contribution from a non-extinguished, soft plasma component with a temperature of 0.2 keV. The figure includes two cases, one with $\theta = 80^\circ$ (top panel) and another with $\theta = 30^\circ$ (bottom panel). Indeed, the model with $\theta = 80^\circ$ exhibits similar properties as those observed in β/δ sources.

It is thus easily argued that in β/δ -type objects, the soft X-ray emission must definitely come from an extended source that is no longer extinguished by the disk. That is, outflows (jets and/or winds) produced by the central symbiotic system. The best example is that of R Aqr which has been detected to have X-ray-emitting jets (Kellogg et al. 2001, 2007) expanding into hot bubbles. In fact, the jets seem to be feeding the most extended X-ray emission (Toalá et al. 2022). Its integrated spectrum including these morphological features, in addition to the central engine, is that of a β/δ -type symbiotic star as discussed in Toalá et al. (2023).

The simulations presented here also suggest that high-accreting symbiotic systems that form a disk, that is, sources in which their boundary layer produce soft X-ray photons (some α -type sources; see Section 2) can only be observed for small θ values, that is pole-on directions from the accretion disk. Otherwise, these cannot be detected for edge-on alignments because their soft X-ray emission would be easily extinguished. It is also worth noticing that not all α sources can be directly associated with thermonuclear burning on the surface of the WD. As example, we mention the case of RR Tel where soft X-ray emission can be best explain by shocked-heated plasma very likely due to winds (González-Riestra et al. 2013). Similarly, the soft X-ray component detected in the 2016 *XMM-Newton* observations of HM Sge was produced by shocked-heated plasma from a jet (Toalá, Botello & Sabin 2023).

β -type sources are typically attributed to the presence of shocks produced by outflows with the extended atmosphere of the red giant companion or the accretion disk. Spectral analysis of β -type sources do not report high column densities in order to produce acceptable fits (see for example the case of V1329 Cyg: Stute et al. 2011), a feature that suggests that these systems are also observed near pole-on from the orbital plane of the binary system. However, we also note that some sources classified as β -type symbiotic stars, that is, sources with the peak of emission at about 1 keV also exhibit high energy tails. Nuñez et al. (2014) classified Hen 2-87 as a β source even after detecting the 6–7 keV Fe feature best seen in the the 2003 *XMM-Newton* observations. In addition, their spectral fit required a relatively high N_H of $\approx 10^{22}$ cm $^{-2}$ to obtain a good fit. This points towards the presence of a reflection component that might have been overlooked in β -type symbiotic systems given the short exposure times of available observations.

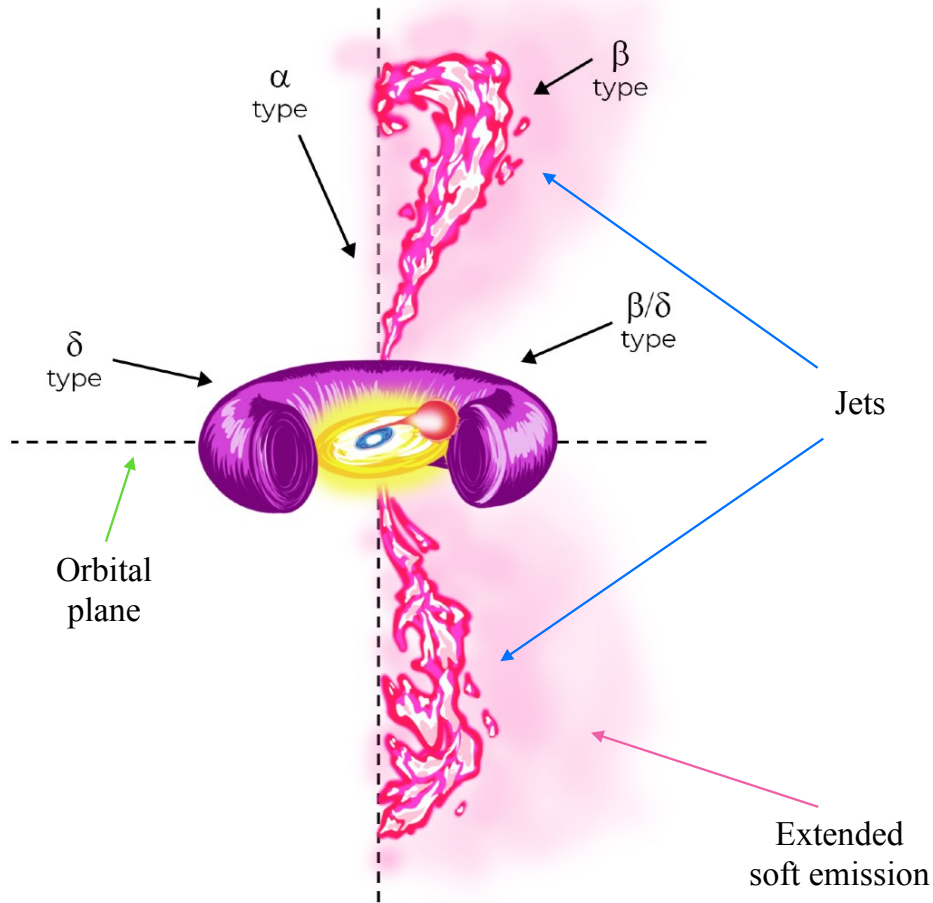


Figure 7. Representation of the morphology of the structures around a symbiotic system. The binary and the accretion disk are located at the centre of the sketch. The left side from the vertical (dashed line) represents a system without extended emission, while the right side is that of a system with the presence of a bipolar ejections (jets). The black arrows and labels (α , β , δ and β/δ) represent line of sights. The structures are not to scale.

There is not much to say regarding γ -type sources, because they have been defined as symbiotic systems hosting neutron stars (see [Merc et al. 2019](#)). However, the evident similarities between X-ray spectra of γ sources with those of the δ -type (see for example [Bozzo et al. 2018](#); [Kaplan et al. 2007](#); [Masetti et al. 2002, 2007](#)) suggest that similar ideas might be invoked to describe symbiotic systems hosting neutron stars. A situation that is out of the scope of the present paper.

To put these ideas into context, we present in Fig. 7 a sketch of the production of the different X-ray-emitting symbiotic types with viewing angle. To explain the β and β/δ sources we require the contribution from extended X-ray-emitting gas such as jets and/or hot bubbles.

There is of course a caveat to the proposed ideas that is worth mentioning, the distribution of material surrounding the symbiotic system. As mentioned before, hydrodynamical simulations have shown that the flared disk is created around the WD component with a relatively small size. Simulations presented in [Lee et al. \(2022\)](#) predict a disk size 0.2 AU, but the rest of the material surrounding the disk and the symbiotic system must have a turbulent toroidal structure extending up to ~ 100 AU ([de Val-Borro et al. 2009](#); [Makita et al. 2000](#); [Liu et al. 2017](#); [Lee et al. 2022](#); [Saladino et al. 2019](#)). Evidently, the next step for this project will be to performed radiative transfer of X-ray photons through density distributions produced by time-dependent hydrodynamic numerical simulations. In addition, we rejected large

opening angle models because the model geometry is not longer that of a disk. But we note that this parameter also depend on the binary properties as demonstrated by the simulations cited above.

4.1 Spectral variability

Multi-epoch observations of symbiotic stars have demonstrated that their spectra change, in some cases dramatically. These clear variations in the spectral shape can also be explained using the results presented in previous sections.

A complex case of spectral variability is that of T CrB, which went from a β -type in quiescent phase with a plasma temperature of ≈ 17 keV ([Kennea et al. 2009](#)) to β/δ -type with a dominant plasma temperature of ≈ 8 keV after entering a super active state ([Luna et al. 2018](#); [Zhekov & Tomov 2019](#)). Different publicly available X-ray spectra obtained from 2017 to 2020 (see Appendix B) show a decrease in soft X-ray emission while the hard X-ray emission increased. [Luna et al. \(2019\)](#) argued that the temperature of the hard component has not changed, only its flux. However, the evident changes in the 2.0–5.0 keV spectral range might suggest that not only the plasma temperature of the hot gas has changes, but other properties as N_{H} and very likely R_{in} . That is, the disk has been experiencing dramatic changes. It is very likely that these have been produce by a disk instability as discussed by [Luna et al. \(2019, 2018\)](#),

but we note that such works suggest that the soft X-ray emission is produced very close to the WD surface, but the simulations presented here cannot support this idea because the soft emission would be easily absorbed by the dense accretion disk. Thus, it is more likely that the soft X-ray emission from T CrB might be produced by winds or jets leaving the densest structure. Another possibility would be that the disk is porous and some of the soft X-ray emission is able to escape before being absorbed. Reflection models tailored to the multi-epoch X-ray observations of T CrB are most needed in order to confirm such strong assertions (Toalá, González-Martín & Sacchi in prep.).

Another interesting source is the very likely symbiotic system Y Gem (see, e.g., Yu et al. 2022). The X-ray data show that reflection is definitely the dominant physics and the extreme spectral variations suggest that the disk has experienced dramatic changes in short periods of time (see the bottom panel of Fig. B1). The earliest observation obtained in 2013 did not detect soft X-ray emission ($E < 1.0$ keV) and does not exhibit the clear presence of the Fe emission lines. This suggest a β -type origin with an extremely large N_{H} . By 2014 November, the source started exhibiting soft X-ray emission ($E < 1.0$ keV) and the appearance of the unresolved contribution from the Fe emission lines. By 2015 the luminosity of the hard component increases whilst maintaining a more or less similar soft flux. Finally, by 2015 the flux of the hard component decreases again. The hard component of Y Gem do not have the same lower energy range, suggesting that the accretion disk density is changing in very short time scales. A reanalysis of the spectra presented in Yu et al. (2022) is most desirable in order to measure the contribution from the reflection component.

Thus far, the best example of the variation of the three Fe emission lines in the 6.0–7.0 keV energy range is that of CH Cyg. Multi-epoch X-ray observations obtained with *ASCA*, *Suzaku*, *Chandra* and *XMM-Newton* obtained from 1994 to 2018 revealed the dramatic flux and equivalent width (EW) changes of the reflection-dominated 6.4 keV line with respect to the 6.7 and 6.79 keV Fe emission lines (Mukai et al. 2007; Toalá et al. 2023). Given that the variations in the EW of the 6.4 keV emission line are expected to be the result of the covering angle Ω and the effective column density N_{H} (see, e.g., Inoue 1985), Toalá et al. (2023) argued that these might be caused by a non-steady mass-loss from the red giant. However, here we also demonstrated that extreme variations in the Fe emission lines can be also produced by varying the plasma temperature of the boundary layer (see Fig. A1). A detailed analysis of the multi-epoch X-ray observations of CH Cyg (and other β/δ sources) is thus needed to unveil the true accretion process and its relationship with the mass-loss ejections from the companion.

5 SUMMARY AND CONCLUSIONS

We presented radiative transfer simulations performed with *SKIRT* of X-ray photons through a flared disk to study the properties of reflection in symbiotic systems. We assume that the source of X-ray photons is the X-ray-emitting plasma at the boundary layer, the region between the accretion disk and the surface of the WD, which is assumed to be thermal in origin. Models presented here adopted a flared disk geometry that is characterised by inner and outer radii R_{in} and R_{out} , effective column density N_{H} and opening angle ϕ . Simulations were produced by changing the input plasma model kT and were convolved with a viewing angle θ where 0° is pole-on view and 90° is edge-on view.

By varying all of the disk parameters, the simulations presented

here reproduce a variety of observed properties in the X-ray spectra of symbiotic systems, in particular for those dominated by reflection. We proposed that in such systems the properties of the accretion disk are fundamental to understand the resultant X-ray spectrum in combination with the viewing angle.

Our main findings can be summarised as follow:

(i) We assumed that the boundary layer is the source of X-ray photons and that it emits as an optically-thin shocked plasma (i.e., thermal in nature). The interaction of these X-ray photons with the accretion disk produces X-ray spectra of the δ -type similarly to previous analysis of reflection physics adopting a power law (non thermal) as input model. Thus, a magnetic field is not necessary to explain hard X-ray emission from symbiotic systems.

(ii) δ -type symbiotic systems are naturally produced by the presence of an accretion disk with close to edge-on viewing angles. The simulations presented here suggest that δ systems are most likely associated with low-accreting symbiotic stars with high-temperature plasma ($kT > 1$ keV) in the boundary layer in order to be detected through their dense disks. Conversely, high-accreting systems, those with soft plasma temperatures in their boundary layers will be difficult to be detected through edge-on viewing angles.

(iii) Using two-temperature plasma models (a hard plus a soft component) as input parameters for the boundary layer cannot reproduce β/δ symbiotic systems. In such cases, the soft X-ray component is easily absorbed by the presence of the disk. Thus, the soft component of the β/δ -type sources can only be explain if this emission corresponds to extended components such as jets, winds and/or hot bubbles.

(iv) Some soft sources of the α type can be detected if their X-ray emission corresponds to extended X-ray-emitting features such as jets, winds and/or hot bubbles outside the line of sight of the accretion disk.

(v) Dramatic spectral variations such as the flux and EW of the Fe emission lines in the 6.0–7.0 keV energy range can be explained by the variable structure of the accretion disk. The intensities of the 6.4, 6.7 and 6.79 keV Fe emission lines are tightly correlated to the increase in the plasma temperature of the boundary layer and to the density of the accretion disk.

(vi) Our models predict that the slope of the very hard X-ray emission ($E > 10$ keV) increases with the plasma temperature of the boundary layer. Higher plasma temperatures are a consequence of low-accreting systems.

We note that we have not tailored our *SKIRT* models to any specific symbiotic system, but the results presented here have helped us unveil the effects of each parameter of the accretion disk and their specific role impacting the X-ray spectra of symbiotic systems. Spectral fits to a sample of X-ray-emitting symbiotic stars is being perform using *SKIRT* reflection models through neural networks (Toalá et al. in prep.). Particular effort will be placed in those with multi-epoch observations as they will help peer into the variable nature of the accretion disks.

Future radiative-transfer calculations performed on more realistic models obtained from time-dependent hydrodynamical numerical simulations will be the next step to corroborate the results presented here.

ACKNOWLEDGEMENTS

The author thanks comments and suggestions from an anonymous referee that improved the presentation of the results and their discus-

sion. The author also thanks O. González-Martín, R. Montez Jr. and M. A. Guerrero for fruitful discussions that resulted in the ideas presented in this work. Special thanks to B. vander Meulen for teaching the author how to use the `SKIRT` code and to J. C. Álvarez from X.i.k. studio for providing the cartoon used in this paper. This work has made a large use of NASA's Astrophysics Data System (ADS).

DATA AVAILABILITY

The data underlying this article will be shared on reasonable request to the corresponding author.

REFERENCES

- Arnaud, K. A. 1996, *Astronomical Data Analysis Software and Systems V*, 101, 17
- Bondi, H. & Hoyle, F. 1944, *MNRAS*, 104, 273.
- Bozzo, E., Bahramian, A., Ferrigno, C., et al. 2018, *A&A*, 613, A22.
- Camps, P. & Baes, M. 2020, *Astronomy and Computing*, 31, 100381.
- Corradi, R. L. M., Ferrer, O. E., Schwarz, H. E., et al. 1999, *A&A*, 348, 978
- de Val-Borro, M., Karovska, M., & Sasselov, D. 2009, *ApJ*, 700, 1148.
- Done, C., Davis, S. W., Jin, C., et al. 2012, *MNRAS*, 420, 1848.
- Eze, R. N. C. 2014, *MNRAS*, 437, 857.
- González-Martín, O., Ramos Almeida, C., Fritz, J., et al. 2023, *A&A*, 676, A73.
- González-Riestra, R., Selvelli, P., & Cassatella, A. 2013, *A&A*, 556, A85.
- Inoue, H. 1985, *Space Sci. Rev.*, 40, 317.
- Ishida, M., Okada, S., Hayashi, T., et al. 2009, *PASJ*, 61, S77.
- Kaplan, D. L., Levine, A. M., Chakrabarty, D., et al. 2007, *ApJ*, 661, 437.
- Kellogg, E., Anderson, C., Korreck, K., et al. 2007, *ApJ*, 664, 1079.
- Kellogg, E., Pedelty, J. A., & Lyon, R. G. 2001, *ApJ*, 563, L151.
- Kennea, J. A., Mukai, K., Sokolowski, J. L., et al. 2009, *ApJ*, 701, 1992.
- Lee, Y.-M., Kim, H., & Lee, H.-W. 2022, *ApJ*, 931, 142.
- Liu, Z.-W., Stancliffe, R. J., Abate, C., et al. 2017, *ApJ*, 846, 117.
- Luna, G. J. M., Nelson, T., Mukai, K., et al. 2019, *ApJ*, 880, 94.
- Luna, G. J. M., Mukai, K., Sokolowski, J. L., et al. 2018, *A&A*, 619, A61.
- Luna, G. J. M., Sokolowski, J. L., Mukai, K., et al. 2013, *A&A*, 559, A6.
- Luna, G. J. M., Sokolowski, J. L., & Mukai, K. 2008, *RS Ophiuchi (2006) and the Recurrent Nova Phenomenon*, 401, 342. doi:10.48550/arXiv.0711.0725
- Luna, G. J. M. & Sokolowski, J. L. 2007, *ApJ*, 671, 741.
- Magdziarz, P., Blaes, O. M., Zdziarski, A. A., et al. 1998, *MNRAS*, 301, 179.
- Magdziarz, P. & Zdziarski, A. A. 1995, *MNRAS*, 273, 837.
- Makita, M., Miyawaki, K., & Matsuda, T. 2000, *MNRAS*, 316, 906.
- Masetti, N., Landi, R., Pretorius, M. L., et al. 2007, *A&A*, 470, 331.
- Masetti, N., Dal Fiume, D., Cusumano, G., et al. 2002, *A&A*, 382, 104.
- Merc, J., Gális, R., & Wolf, M. 2019, *Astronomische Nachrichten*, 340, 598.
- Mukai, K. 2017, *PASP*, 129, 062001.
- Mukai, K., Ishida, M., Kilbourne, C., et al. 2007, *PASJ*, 59, 177.
- Mürset, U., Wolff, B., & Jordan, S. 1997, *A&A*, 319, 201
- Núñez, N. E., Luna, G. J. M., Pillitteri, I., et al. 2014, *A&A*, 565, A82. doi:10.1051/0004-6361/201322999
- Orio, M., Luna, G. J. M., Kotulla, R., et al. 2017, *MNRAS*, 470, 2212.
- Orio, M., Zezas, A., Munari, U., et al. 2007, *ApJ*, 661, 1105.
- Ortiz, R. & Guerrero, M. A. 2021, *ApJ*, 912, 93.
- Patterson, J. & Raymond, J. C. 1985, *ApJ*, 292, 535.
- Podsiadlowski, P. & Mohamed, S. 2007, *Baltic Astronomy*, 16, 26
- Pringle, J. E. & Savonije, G. J. 1979, *MNRAS*, 187, 777.
- Saladino, M. I., Pols, O. R., & Abate, C. 2019, *A&A*, 626, A68.
- Saeedi, S., Sasaki, M., & Ducci, L. 2018, *MNRAS*, 473, 440.
- Stute, M., Luna, G. J. M., & Sokolowski, J. L. 2011, *ApJ*, 731, 12.
- Toalá, J. A., Botello, M. K., & Sabin, L. 2023, *ApJ*, 948, 14.
- Toalá, J. A., González-Martín, O., Karovska, M., et al. 2023, *MNRAS*, 522, 6102.
- Toalá, J. A., Sabin, L., Guerrero, M. A., et al. 2022, *ApJ*, 927, L20.

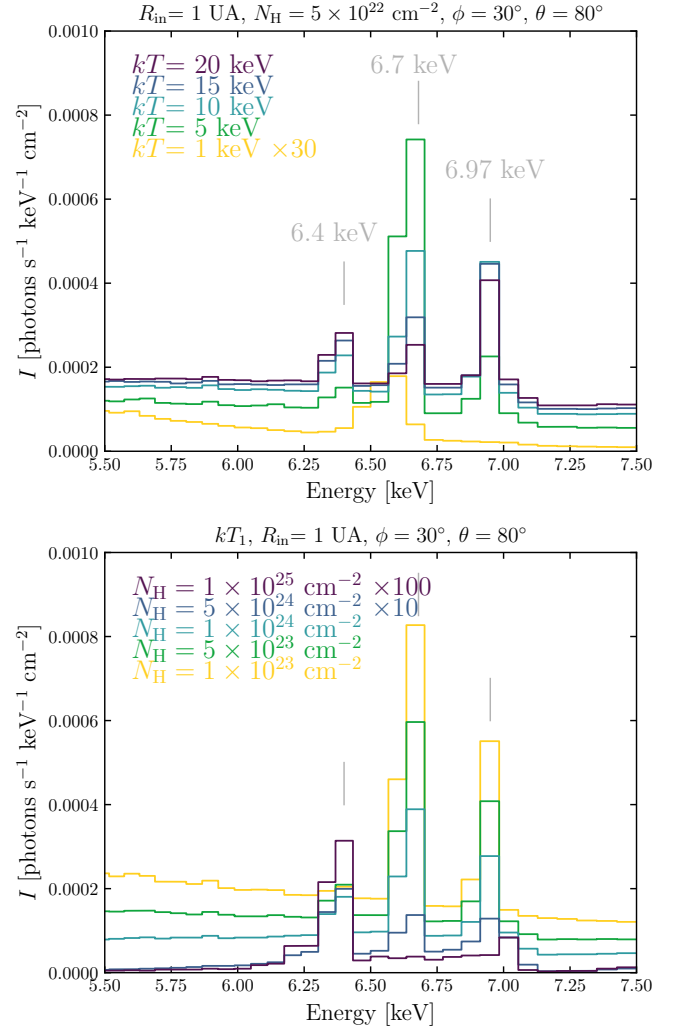


Figure A1. Impact on the the three Fe emission lines produced by the plasma temperature kT (top panel) and the column density N_H . The 6.4, 6.7 and 6.79 keV Fe emission lines are marked with grey vertical segments.

- Trayford, J. W., Camps, P., Theuns, T., et al. 2017, *MNRAS*, 470, 771.
- Vander Meulen, B., Camps, P., Stalevski, M., et al. 2023, *A&A*, 674, A123.
- Wheatley, P. J. & Kallman, T. R. 2006, *MNRAS*, 372, 1602.
- Wheatley, P. J., Mukai, K., & de Martino, D. 2003, *MNRAS*, 346, 855.
- Yu, Z.-li., Xu, X.-jie., Shao, Y., et al. 2022, *ApJ*, 932, 132.
- Zhekov, S. A. & Tomov, T. V. 2019, *MNRAS*, 489, 2930.

APPENDIX A: IRON LINES

Here we present details of spectra presented in the bottom right panel of Fig. 4 and the bottom panel of Fig. 5 to highlight the changes in the flux of the 6.4, 6.7 and 6.97 keV Fe emission lines. These variations are produced by the plasma temperature kT (top panel of Fig. A1) and the flared disk column density N_H (bottom panel of Fig. A1).

APPENDIX B: X-RAY SPECTRA OF SYMBIOTIC STARS

For means of discussion, here we present publicly available X-ray spectra of four symbiotic stars. Fig. B1 presents multi-epoch *Chan-*

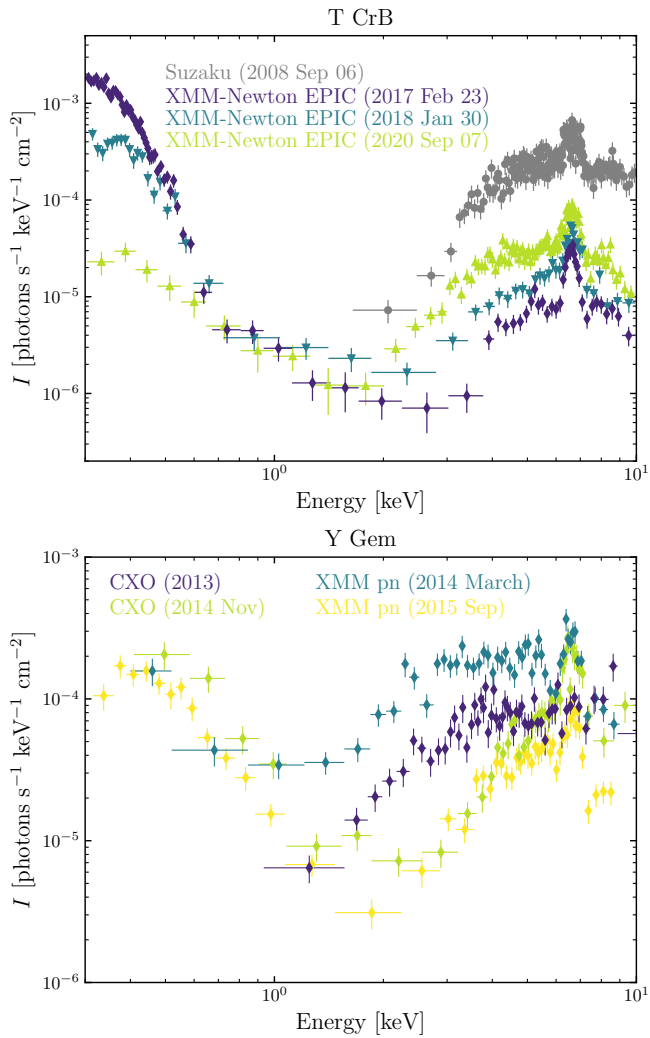


Figure B1. X-ray spectra of symbiotic systems obtained from publicly available archives. The panels show spectra from T CrB (top) and Y Gem (bottom).

dra, *XMM-Newton* and *Suzaku* observations of the β/δ -type object T CrB. We note that the observations of T CrB have been analysed in [Kennea et al. \(2009\)](#), [Luna et al. \(2018\)](#) and [Zhekov & Tomov \(2019\)](#) except that obtained in 2020. The bottom right panel shows multi-epoch observations of Y Gem, a source that has been studied in the framework of AGB stars with UV/X-ray excess (see [Ortiz & Guerrero 2021](#), and references therein), however, it is very likely that this is a misclassified symbiotic star as recently suggested by [Yu et al. \(2022\)](#).